Modified DFT Filter Banks with Perfect Reconstruction

Tanja Karp, *Member, IEEE,* and N. J. Fliege, *Senior Member, IEEE*

***Abstract*— In this paper, essential features of the recently introduced modified discrete Fourier transform DFT (MDFT) filter bank are presented. First, it is shown that all analysis and synthesis filters—obtained by appropriate complex modulation of a low-pass prototype filter—are linear phase. This is important for subband image coding applications. Another important property is the structure-inherent alias cancellation: all odd alias spectra are automatically compensated in the synthesis filter bank. Further on, the MDFT filter bank provides perfect reconstruction for the same prototypes as for cosine-modulated filter banks. Thus, the same design methods can be used. Finally, different mappings of the input signal into the subbands are discussed and a comparison to the well-known cosine-modulated filter banks is given.**

***Index Terms*—Complex modulation, linear-phase analysis and synthesis filters, modulated filter bank, perfect reconstruction, pseudo-QMF design.**

I. Introduction

DIGITAL filter banks have found wide applications and are particularly useful in subband coding and multiple carrier data transmission. In both applications, critically decimated M-channel analysis and synthesis filter banks are used. Among a great number of different filter-bank approaches, cosine-modulated filter banks have become very popular and have been developed to provide perfect reconstruction (PR), e.g., [1]–[5]. Another popular filter bank, namely the discrete Fourier transform (DFT) polyphase filter bank [6], providing highest computational efficiency, suffers from the fact that it is not able to cancel alias components caused by subsampling the subband signals. This disadvantage has been overcome by introducing a certain modification which leads to the modified DFT (MDFT) filter bank [7]–[9].

In this paper, essential features of the MDFT filter bank are presented and compared to the cosine-modulated filter bank. In Section II, it is shown that the MDFT filter bank is able to provide linear phase in both, analysis and synthesis part, independently. Furthermore, it is shown that the MDFT filter bank has a structure inherent alias cancellation: all odd alias spectra are automatically compensated. In Section III, the MDFT filter bank is applied with almost PR utilizing the pseudo-quadrature mirror filter (QMF) principle. In Section IV, it is shown that the MDFT filter bank can even be designed to provide PR. Although the MDFT filter bank is particularly suitable for processing complex-valued signals, there also exist mappings for real input signals into complex subband signals which are described in Section V. Finally, in Section VI, the MDFT filter bank is compared to the cosine-modulated filter bank.

Manuscript received August 21, 1996; revised October 20, 1997. This paper was recommended by Associate Editor T. Q. Nguyen.

The authors are with the University of Mannheim, 68131 Mannheim, Germany.

Publisher Item Identifier S 1057-7130(99)09223-X.

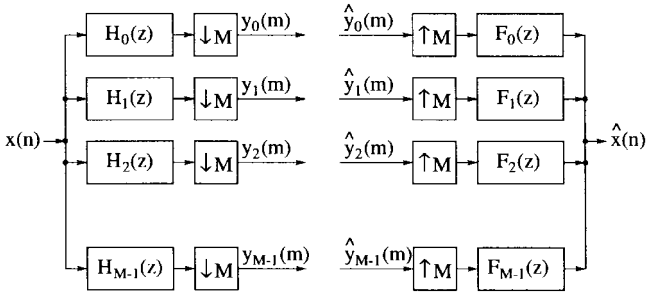

Fig. 1. Complex modulated filter bank.

II. MDFT Filter Banks

MDFT filter banks are modified complex modulated, critically subsampled filter banks based on DFT filter banks. They combine key features of DFT filter banks as linear phase analysis and synthesis filters and an efficient realization with almost PR or PR.

In this section we will first recall the characteristics of DFT filter banks and then show how MDFT filter banks can be derived by introducing of some modifications. Due to these modifications a structure inherent alias cancellation is obtained yielding almost PR or PR.

A. DFT Filter Banks

Fig. 1 shows an M-channel DFT filter bank. $H_k(z)$ and $F_k(z)$ are the analysis and synthesis filters, respectively. $\boxed{\downarrow M}$ describes a decimation of the sampling rate by the factor M and $\boxed{\uparrow M}$ the corresponding expander.

1) Modulated Linear-Phase Analysis and Synthesis Filters: One of the key features of DFT filter banks is the ability to realize linear-phase analysis and synthesis filters by means of an appropriate complex modulation of a low-pass prototype filter. To achieve this, we derive the modulated filters $h_k(n)$ and $f_k(n)$ in two steps. In a first step, from a real-valued zero-phase low-pass prototype filter $p(n)$ with a transition band from $-\pi/M$ to π/M, we derive complex modulated zero-phase filters

$$p_k(n) = p(n)W_M^{-kn}, \quad k = 0, \cdots, M-1 \tag{1}$$

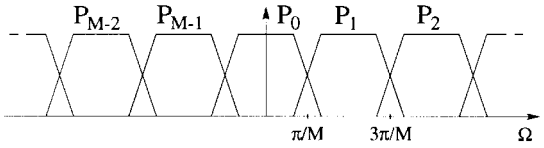

Fig. 2. Frequency response of the filters $P_k(e^{j\Omega})$.

with $W_M^k = \exp[-j(2\pi k/M)]$, which, in the z domain, corresponds to

$$P_k(z) = P(zW_M^k), \quad \text{where} \quad \mathcal{Z}\{p(n)\} = P(z). \tag{2}$$

Substituting z by $e^{j\Omega}$, we obtain the frequency representation of $p_k(n)$

$$P_k(e^{j\Omega}) = P(e^{j(\Omega-\Omega_k)}), \quad \Omega_k = \frac{2\pi k}{M}. \tag{3}$$

From (3), it is obvious that the filters $P_k(e^{j\Omega})$ are frequency shifted versions of the prototype filter $P(e^{j\Omega}) = P_0(e^{j\Omega})$ (see Fig. 2).

In order to obtain causal analysis and synthesis filters, the impulse responses $p_k(n)$ are delayed by $(N-1)/2$ samples. Hence, the time-domain representation of the analysis filters is

$$\begin{aligned} h_k(n) &= p_k\left(n - \frac{N-1}{2}\right) \\ &= p\left(n - \frac{N-1}{2}\right) W_M^{-k(n-(N-1)/2)}, \\ & \qquad n = 0, \cdots, N-1, \quad k = 0, \cdots, M-1. \end{aligned} \tag{4}$$

The synthesis filters $f_k(n)$ are supposed to be identical to the analysis filters

$$f_k(n) = h_k(n), \quad n = 0, \cdots, N-1, \quad k = 0, \cdots, M-1. \tag{5}$$

Mapping (4) and (5) into the z domain and into the frequency domain yields

$$\begin{aligned} H_k(z) &= F_k(z) \\ &= z^{-((N-1)/2)} P_k(z) \\ &= z^{-((N-1)/2)} P(zW_M^k) \end{aligned} \tag{6}$$

$$\begin{aligned} H_k(e^{j\Omega}) &= F_k\left(e^{j\Omega}\right) \\ &= e^{-j\Omega((N-1)/2)} P_k\left(e^{j\Omega}\right) \\ &= e^{-j\Omega((N-1)/2)} P\left(e^{j(\Omega-\Omega_k)}\right). \end{aligned} \tag{7}$$

From (7), we see directly that all analysis and synthesis filters are linear phase if the low-pass prototype $p(n)$ satisfies the zero-phase property.

2) Realization as a DFT Polyphase Filter Bank: Bellanger *et al.* have shown in [6] that complex modulated filter banks can be realized efficiently by DFT polyphase filter banks. Fig. 3 shows the polyphase realization of the analysis filter bank. $G_k(z)$ denotes the kth type-1 polyphase filter of the low-pass filter $H_0(z)$ and reads in the time domain

$$g_k(m) = h_0(m \cdot M + k), \quad k = 0, \cdots M-1.$$

The factor $W_M^{k((N-1)/2)}$ in the kth band of the filter bank in Fig. 3 is due to the phase of the modulation caused by the time delay of the prototype filter by $(N-1)/2$ samples [see (4)]. The inverse DFT (IDFT) only realizes the modulation by W_M^{-kn}.

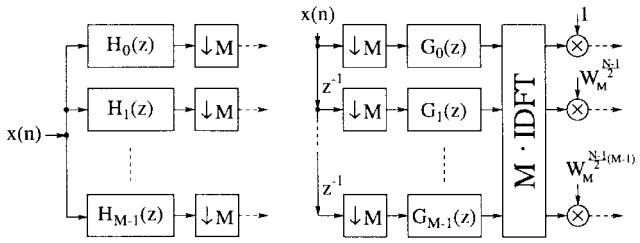

Fig. 3. DFT polyphase realization of a complex modulated analysis filter bank.

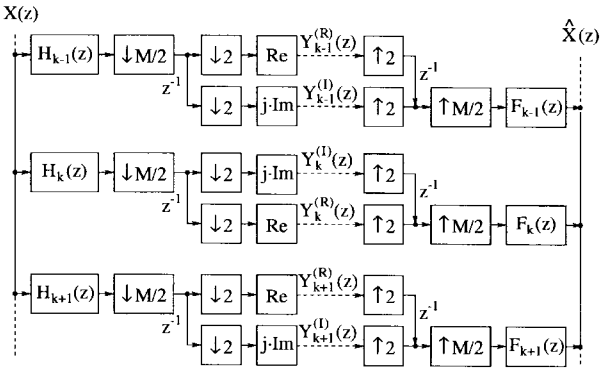

Fig. 4. Modified DFT filter bank.

B. Structure-Inherent Alias Cancellation of MDFT Filter Banks

Although DFT polyphase filter banks as shown in Fig. 3 are of highest computational efficiency and, therefore, particularly useful for practical implementations, this kind of filter bank is not suitable to subband coding applications since no aliasing is cancelled within the DFT filter bank. This disadvantage will be overcome by introducing the following modifications for the MDFT filter bank.

The MDFT filter bank is a complex modulated M-channel filter bank, with a two-step decimation of the subband signals. Upon decimating the sampling rate by the factor $M/2$ (M must be even), another decimation by two is realized with and without a delay of one sampling period.

In the subbands, either the real or the imaginary part is used, respectively. Fig. 4 shows a detail of this filter bank. The impulse responses of the linear-phase analysis and synthesis filters $H_k(z)$ and $F_k(z)$ are given in (4) and (5), respectively.

The MDFT filter bank is critically sampled. In case of complex valued input data $x(n)$, a sequence of M input samples is mapped into M real and M imaginary subband signals at a sampling rate reduced by M. For real input signals, half of the subband signals are either complex conjugates of the others or zero as will be shown in Section V, and therefore remain unused.

In this section, we demonstrate that not only adjacent alias spectra but all odd alias spectra are compensated within the MDFT filter bank. The alias cancellation is independent of the prototype filter design and only depends on the structure of

the MDFT filter bank. This property will be used later on to derive pseudo-QMF and PR conditions on MDFT filter banks. In order to describe aliasing terms and distortions produced by the MDFT filter bank we have to express the reconstructed signal $\hat{X}(z)$ in terms of the input signal $X(z)$.

First, the input signal is divided into subband signals $X_k^{(R)}(z^M)$ and $X_k^{(I)}(z^M)$. Within the analysis filter bank, we especially look at the effects of the modifications introduced by the MDFT filter bank:

1) decimation of the subband signals without and with a delay;
2) taking alternately the real and imaginary part of the subband signals.

The input signal $x(n)$ is complex valued

$$x(n) = x_R(n) + j \cdot x_I(n) \tag{8}$$

and its z-transform can be written as

$$X(z) = X^{(R)}(z) + X^{(I)}(z) \tag{9}$$

where the real and imaginary part of $x(n)$ have been transformed separately

$$X^{(R)}(z) = \mathcal{Z}\{x_R(n)\}$$
$$X^{(I)}(z) = \mathcal{Z}\{j \cdot x_I(n)\}.$$

Let us also define

$$\overline{X}(z) = X^{(R)}(z) - X^{(I)}(z). \tag{10}$$

In a first step, we ignore the sampling rate decimation in the subbands and just examine the consequences of taking the real and imaginary part, respectively[1]

$$\begin{aligned}
&\mathrm{Re}\{h_k(n) * x(n)\} \\
&\quad = \tfrac{1}{2}[h_k(n) + h_k^*(n)] * x_R(n) \\
&\qquad + \tfrac{1}{2}[h_k(n) - h_k^*(n)] * j \cdot x_I(n) \\
&\quad = \tfrac{1}{2}[h_k(n) \pm h_{M-k}(n)] * x_R(n) \\
&\qquad + \tfrac{1}{2}[h_k(n) \mp h_{M-k}(n)] * j \cdot x_I(n) \qquad (11) \\
&j\ \mathrm{Im}\{h_k(n) * x(n)\} \\
&\quad = \tfrac{1}{2}[h_k(n) - h_k^*(n)] * x_R(n) \\
&\qquad + \tfrac{1}{2}[h_k(n) + h_k^*(n)] * j \cdot x_I(n) \\
&\quad = \tfrac{1}{2}[h_k(n) \mp h_{M-k}(n)] * x_R(n) \\
&\qquad + \tfrac{1}{2}[h_k(n) \pm h_{M-k}(n)] * j \cdot x_I(n). \qquad (12)
\end{aligned}$$

Here, we have used the fact that the following relation between the impulse responses of $h_{M-k}(n)$ and $h_k^*(n)$ holds true due to (4)[2]

$$h_k^*(n) = \begin{cases} h_{M-k}(n), & \text{odd } N \\ -h_{M-k}(n), & \text{even } N. \end{cases} \tag{13}$$

[1] "$x(n) * y(n)$" denotes the convolution between $x(n)$ and $y(n)$ and $h_k^*(n)$ denotes the conjugate complex of $h_k(n)$.

[2] For $k = 0$ $h_{M-k}(n) = h_M(n)$ has to be interpreted as $h_0(n)$.

Taking (9) and (10) into account, (11) and (12) can be expressed in the z domain as follows:

$$\begin{aligned}
&\mathcal{Z}\{\mathrm{Re}\{h_k(n) * x(n)\}\} \\
&\quad = \tfrac{1}{2}[H_k(z) \pm H_{M-k}(z)]X^{(R)}(z) \\
&\qquad + \tfrac{1}{2}[H_k(z) \mp H_{M-k}(z)]X^{(I)}(z) \\
&\quad = \tfrac{1}{2}\left[H_k(z)X(z) \pm H_{M-k}(z)\overline{X}(z)\right] \qquad (14) \\
&\mathcal{Z}\{\mathrm{Im}\{h_k(n) * x(n)\}\} \\
&\quad = \tfrac{1}{2}[H_k(z) \mp H_{M-k}(z)]X^{(R)}(z) \\
&\qquad + \tfrac{1}{2}[H_k(z) \pm H_{M-k}(z)]X^{(I)}(z) \\
&\quad = \tfrac{1}{2}\left[H_k(z)X(z) \mp H_{M-k}(z)\overline{X}(z)\right]. \qquad (15)
\end{aligned}$$

Next, let us regard the decimation of the sampling rate. We know from [10] that the following relationship between a signal $a(n)$ and the decimated signal $b(m) = a(m \cdot M + \lambda)$ exists in the z domain (λ denotes the phase offset of the decimation):

$$z^{-\lambda}B(z^M) = \frac{1}{M}\sum_{l=0}^{M-1} A(zW_M^l)W_M^{\lambda l}. \tag{16}$$

One of the modifications in the MDFT filter bank in Fig. 4 is the two step decimation of the subbands. The upper branch of each subband is decimated by the factor M without a phase offset (i.e., without a delay). This corresponds to $\lambda = 0$ in (16). In the lower branch, we can move the delay operation z^{-1} through the first decimation by $M/2$. We thus see that in the lower branch a decimation by M with delay of $M/2$ samples is performed corresponding to a phase offset of $\lambda = -M/2$.

In the following, we assume, without loss of generality, that the real (imaginary) part is taken in the upper undelayed branch of all even (odd) subbands. Applying (16) to (14) and (15) and selecting the appropriate relations for odd and even k, we obtain for the M upper undelayed branches

$$\begin{aligned}
Y_k^{(R)}(z^M) = \frac{1}{2M}\sum_{l=0}^{M-1} &\left[H_k(zW_M^l)X(zW_M^l)\right. \\
&\left.\pm H_{M-k}(zW_M^l)\overline{X}(zW_M^l)\right] \ k \text{ even} \qquad (17) \\
Y_k^{(I)}(z^M) = \frac{1}{2M}\sum_{l=0}^{M-1} &\left[H_k(zW_M^l)X(zW_M^l)\right. \\
&\left.\mp H_{M-k}(zW_M^l)\overline{X}(zW_M^l)\right] \ k \text{ odd}. \qquad (18)
\end{aligned}$$

For the remaining M subband signals in the lower branches, the factor $W_M^{-lM/2}$ occurs in the spectrum of the lth modulation component, corresponding to a phase offset of $\lambda = -M/2$ in (16). We have to take the real part for odd k and the imaginary part for even k, yielding

$$\begin{aligned}
Y_k^{(R)}(z^M) = \frac{z^{-M/2}}{2M}\sum_{l=0}^{M-1} &\left[H_k(zW_M^l)X(zW_M^l)\right. \\
&\left.\pm H_{M-k}(zW_M^l)\overline{X}(zW_M^l)\right]W_M^{-lM/2}, \quad k \text{ odd} \qquad (19) \\
Y_k^{(I)}(z^M) = \frac{z^{-M/2}}{2M}\sum_{l=0}^{M-1} &\left[H_k(zW_M^l)X(zW_M^l)\right. \\
&\left.\mp H_{M-k}(zW_M^l)\overline{X}(zW_M^l)\right]W_M^{-lM/2}, \quad k \text{ even}. \qquad (20)
\end{aligned}$$

After encoding, storing and/or transmitting, and decoding the subband signals, the original input signal $X(z)$ has to be reconstructed in the synthesis filter bank, resulting in an output signal $\hat{X}(z) = \sum_{k=0}^{M-1} \hat{X}_k$, where $\hat{X}_k$ denotes the output signal of the kth synthesis filter

$$\hat{X}_k(z) = F_k(z)\Big[z^{-M/2}Y_k^{(R)}(z^M) + Y_k^{(I)}(z^M)\Big],\ k \text{ even} \tag{21}$$

$$\hat{X}_k(z) = F_k(z)\Big[Y_k^{(R)}(z^M) + z^{-M/2}Y_k^{(I)}(z^M)\Big],\ k \text{ odd}. \tag{22}$$

If we substitute (17) and (20) for $Y_k^{(R)}(z^M)$ and $Y_k^{(I)}(z^M)$, respectively, in (21), and (18) and (19) in (22), and take $W_M^{-lM/2} = (-1)^l$ into account, we get

$$\begin{aligned}\hat{X}_k(z) = {} & \frac{z^{-M/2}}{M} F_k(z) \sum_{l=0}^{M/2-1} \big[H_k(zW_M^{2l})X(zW_M^{2l}) \\ & \pm H_{M-k}(zW_M^{2l+1})\overline{X}(zW_M^{2l+1})\big], \quad k \text{ even} \\ \hat{X}_k(z) = {} & \frac{z^{-M/2}}{M} F_k(z) \sum_{l=0}^{M/2-1} \big[H_k(zW_M^{2l})X(zW_M^{2l}) \\ & \mp H_{M-k}(zW_M^{2l+1})\overline{X}(zW_M^{2l+1})\big], \quad k \text{ odd}.\end{aligned}$$

The reconstructed signal $\hat{X}(z)$ is the sum of all channel output signals $\hat{X}_k(z)$, $k = 0, \cdots, M-1$:

$$\begin{aligned}\hat{X}(z) = {} & \frac{z^{-M/2}}{M} \sum_{k=0}^{M-1} F_k(z) \sum_{l=0}^{M/2-1} \big[H_k(zW_M^{2l})X(zW_M^{2l}) \\ & \pm (-1)^k H_{M-k}(zW_M^{2l+1})\overline{X}(zW_M^{2l+1})\big]. \end{aligned} \tag{23}$$

The second expression of this sum is equal to zero. In order to prove this, we express the analysis and synthesis filters by the common prototype filter [see (6)] and carry out the following modifications:

$$\begin{aligned}& \frac{z^{-M/2}}{M} \sum_{k=0}^{M-1} F_k(z) \sum_{l=0}^{M/2-1} (-1)^k H_{M-k}(zW_M^{2l+1})\overline{X}(zW_M^{2l+1}) \\ & = \frac{z^{-(N-1+M/2)}}{M} \sum_{k=0}^{M-1} P(zW_M^k) \sum_{l=0}^{M/2-1} (-1)^k \\ & \quad \cdot P(zW_M^{2l+1+M-k})\overline{X}(zW_M^{2l+1}) \\ & = \frac{z^{-(N-1+M/2)}}{M} \sum_{l=0}^{M/2-1} \overline{X}(zW_M^{2l+1}) \\ & \quad \cdot \left[\sum_{k=0}^{M/2-1} P(zW_M^{2k})P(zW_M^{2l+1-2k}) \right. \\ & \quad \left. - \sum_{k=0}^{M/2-1} P(zW_M^{2k+1})P(zW_M^{2l-2k})\right].\end{aligned}$$

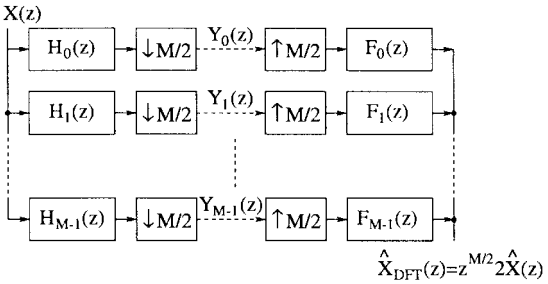

Fig. 5. Complex modulated M-channel filter bank with a subsampling factor of $M/2$.

Substituting $l-k$ for k in the last sum leads to the desired result

$$\begin{aligned}& \frac{z^{-(N-1+M/2)}}{M} \sum_{l=0}^{M/2-1} \overline{X}(zW_M^{2l+1}) \\ & \quad \cdot \left[\sum_{k=0}^{M/2-1} P(zW_M^{2k})P(zW_M^{2l+1-2k}) \right. \\ & \quad \left. - \sum_{k=0}^{M/2-1} P(zW_M^{2k})P(zW_M^{2l+1-2k})\right] = 0.\end{aligned}$$

Note that we do not have to change the start and stop value of the summation index k in the second sum when substituting $l-k$ for k, since the summation covers a whole period of W_M^{2l-2k} and W_M^{2k+1}.

Hence, $\hat{X}(z)$ can be rewritten as

$$\hat{X}(z) = \frac{z^{-M/2}}{M} \sum_{k=0}^{M-1} \sum_{l=0}^{M/2-1} F_k(z)H_k(zW_M^{2l})X(zW_M^{2l}). \tag{24}$$

By this, we have shown that all odd aliasing terms of $\hat{X}(z)$ are compensated. The remaining even alias spectra are the same as in a noncritically decimated DFT filter bank with M channels and a sampling rate decimation of $M/2$, shown in Fig. 5. Its output signal $\hat{X}_{\mathrm{DFT}}(z)$ is given by

$$\hat{X}_{\mathrm{DFT}}(z) = \frac{2}{M} \sum_{k=0}^{M-1} \sum_{l=0}^{M/2-1} F_k(z)H_k(zW_M^{2l})X(zW_M^{2l}). \tag{25}$$

Both output signals $\hat{X}(z)$ and $\hat{X}_{\mathrm{DFT}}(z)$ only differ in a scaling factor and an additional time delay in the MDFT filter bank.

C. Realization as a Modified DFT Polyphase Filter Bank

As shown in [7] the MDFT filter bank can be realized by means of two DFT polyphase filter banks where one is delayed by $M/2$ samples (see Fig. 6). The implementation cost is twice the implementation cost of the DFT filter bank but can be further reduced [11].

III. Almost Perfect Reconstruction

In the following we describe how MDFT filter banks can be designed in such a way that they provide almost PR. Almost PR means that alias distortion as well as linear amplitude and phase distortions can be kept arbitrarily small. The key for the

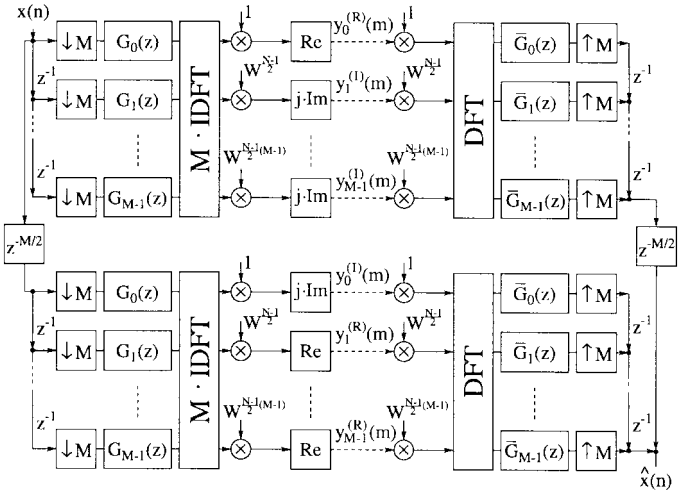

Fig. 6. MDFT filter bank realized by two DFT polyphase filter banks.

filter bank design with almost PR is the pseudo-QMF principle to be discussed next.

A. Pseudo-QMF Filter Bank Design

The design of filter banks utilizing the pseudo-QMF principle has been proposed by several authors, e.g., [12]–[15]. Originally, cosine-modulated filter banks are used with the following features.

1) The filter bank channels are formed by a series of equidistant frequency shifts of an appropriate prototype filter. The transfer functions of adjacent channels must be approximately power complementary between their center frequencies.
2) Only the directly adjacent alias spectra are compensated by an appropriate mechanism.
3) All other alias spectra are suppressed by a sufficiently high stopband attenuation of the prototype filter.

Obviously, the MDFT filter bank is suitable to meet these items. As shown in the preceding section, all odd alias spectra cancel automatically, i.e., independent of the filter characteristic in the MDFT synthesis filter bank, including the first or directly adjacent alias spectra. Thus, the MDFT filter bank meets the second property of pseudo-QMF filter banks.

The approximation quality of the power complementarity of adjacent channels and the stopband attenuation depend on the prototype filter design. The first causes amplitude distortion, the second determines the aliasing distortion. The MDFT filter bank is free from phase distortions since all filters are linear phase with the same group delay. Next, we consider objective functions for the remaining amplitude distortion and aliasing.

B. Amplitude Distortion and Aliasing

In order to describe the remaining amplitude and aliasing distortions, an amplitude distortion function and an aliasing distortion function are presented in the following. Disregarding the alias spectra, an overall transfer function from the input to the output of the filter bank can be obtained [10], [16], which depends on the analysis filters $H_k(z)$ and synthesis

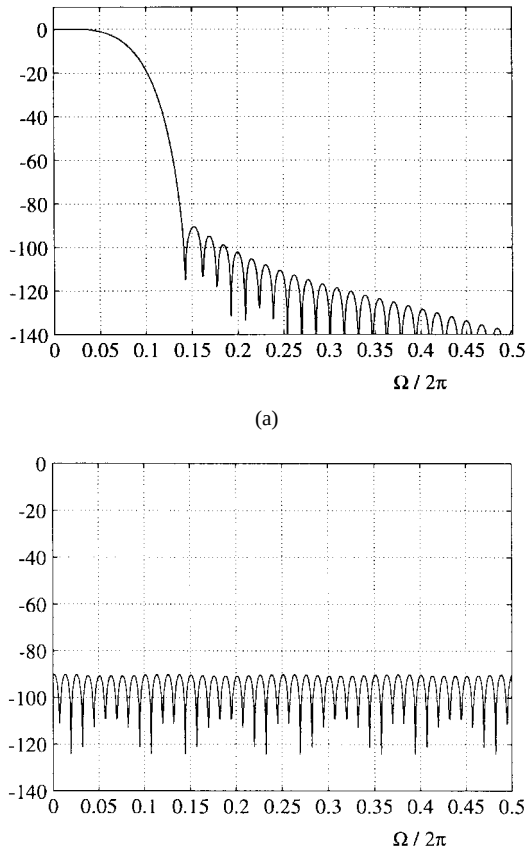

Fig. 7. Frequency response of (a) an optimized Blackman-windowed prototype filter with 65 coefficients for an 8-channel filter bank and (b) the resulting distortion function.

filters $F_k(z),\ k = 0, 1, \cdots, M-1$

$$T_{\text{dist}}(z) = \frac{1}{M} \sum_{k=0}^{M-1} F_k(z) \cdot H_k(z). \tag{26}$$

The distortion function $T_{\text{dist}}(z)$ has linear phase in case of the MDFT filter bank. The corresponding magnitude frequency response should approximate unity at all frequencies

$$|T_{\text{dist}}(e^{j\Omega})| \approx 1, \quad 0 \le \Omega \le 2\pi. \tag{27}$$

Aliasing distortion is described by an appropriate aliasing function. In general, we have aliasing from $M-1$ neighbor subbands with independent signals. Therefore, we have to add the alias components independently. The aliasing function introduced in [10], [16], writes

$$T_{\text{alias}}(z) = \left(\sum_{\ell=1}^{M-1} \left| \frac{1}{M} \sum_{k=0}^{M-1} F_k(z) \cdot H_k\left(zW_M^{\ell}\right) \right|^2 \right)^{1/2}. \tag{28}$$

In the sense of low aliasing distortion, $|T_{\text{alias}}(e^{j\Omega})|$ should tend to zero at all frequencies.

C. Filter-Bank Design

In [17], a design method for MDFT filter banks has been presented. It is based on square-root raised-cosine filters and

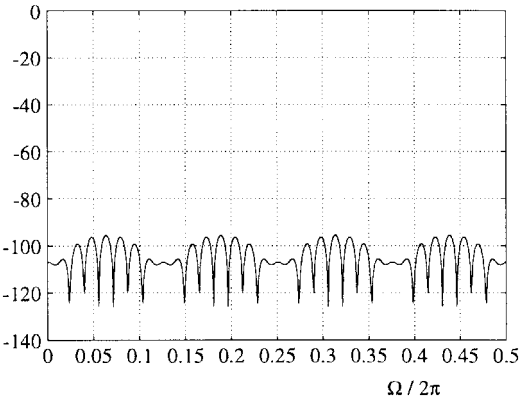

(a)

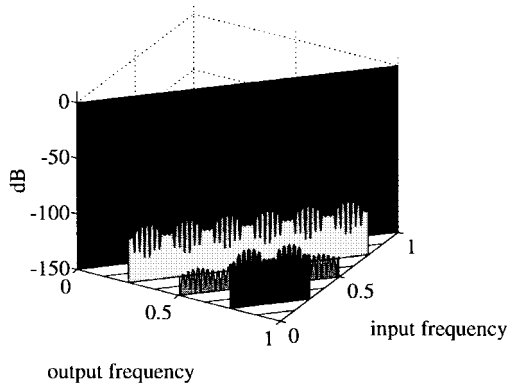

(b)

Fig. 8. (a) Aliasing function and (b) bifrequency representation of the frequency response and aliasing components of the optimized 8-channel filter bank.

provides almost PR. The remaining amplitude and aliasing distortions can be kept arbitrarily small by choosing an appropriate length N of the prototype filter $p(n)$.

After truncating and time-shifting the zero-phase square-root raised-cosine impulse response, it is weighted with a Hamming or Blackman window. Finally, by means of some iteration steps, the frequency response is optimized toward the power-complementary characteristic while keeping the stopband attenuation high.

As an example, we consider an 8-channel ($M = 8$) MDFT filter bank. For a prototype filter length of 65 coefficients, we obtain the frequency response of the prototype filter, shown in Fig. 7(a).

Since the described design method optimizes the power complementary property of the prototype filter, the amplitude distortion (deviation from unity in dB) is very small, i.e., less than -90 dB at all frequencies [see Fig. 7(b)].

Fig. 8(a) shows the aliasing function according to (28) in decibels. The summed-up aliasing power is at least 95-dB below the signal power. Finally, in Fig. 8(b) the bifrequency representation of the frequency responses and alias components of the filter bank are plotted (frequency axis is normalized by the sampling frequency). This plot displays very well the small aliasing and the fact that all odd-indexed alias spectra disappear.

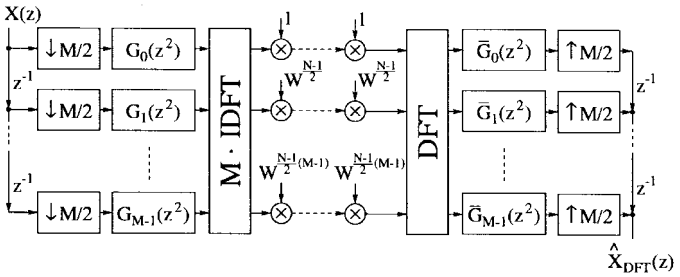

Fig. 9. DFT polyphase realization of the filter bank in Fig. 5.

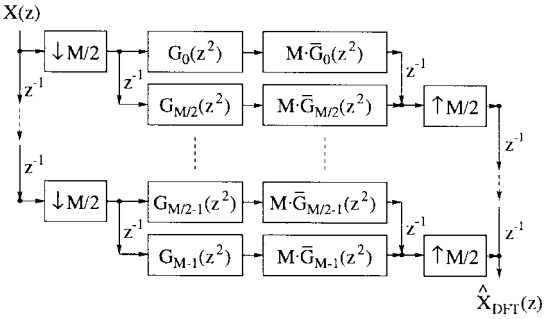

Fig. 10. Simplified structure of Fig. 9 if $N = r \cdot M + 1$.

IV. Perfect Reconstruction

The results of Section II have shown that the output signal of the MDFT filter bank and of the noncritically subsampled filter bank in Fig. 5 only differ in a scaling factor of the amplitude and a time delay. Hence, it is sufficient to regard the noncritically subsampled DFT filter bank with respect to PR. This simplifies the following considerations as we are not required to take the real and imaginary parts, respectively, in the subbands any longer.

For PR, the following conditions have to be satisfied by the filter bank:

1) exact compensation of aliasing;
2) no phase and amplitude distortion.

In order to impose conditions for PR on the analysis and synthesis filters in Fig. 5, it is useful to regard the polyphase realization of the DFT filter bank. In the analysis filter bank, type-1 polyphase filters of the low-pass filter $h_0(n)$ are used

$$g_k(m) = h_0(m \cdot M + k), \quad k = 0, \cdots M-1$$

and in the synthesis filter bank, we use type-3 polyphase filters [10], [18]

$$\overline{g}_k(m) = h_0(m \cdot M - k), \quad k = 0, \cdots M-1.$$

Fig. 9 shows the polyphase realization of the filter bank in Fig. 5.

The multiplications by $W_M^{k(N-1)/2}$ between the IDFT and DFT operations are due to the causality of the analysis and synthesis filters. Remember that the symmetrical, zero-phase prototype filter was first modulated and then time shifted.

A. Analysis and Synthesis Filters of Length $N = r \cdot M + 1$

For the sake of simplicity, let us regard prototypes of length $N = r \cdot M + 1$, $r \in \mathbb{N}$, first. The multiplication with

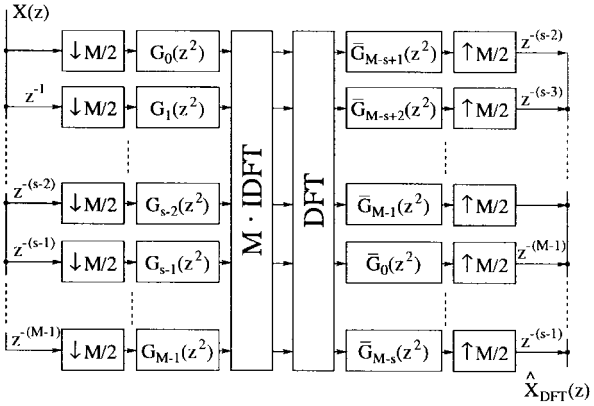

Fig. 11. Simplified polyphase structure for $N = r \cdot M + s$.

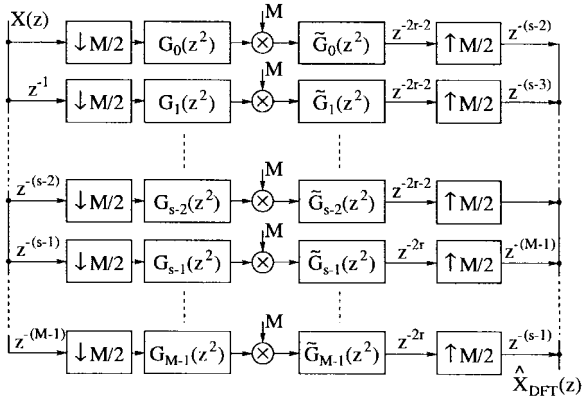

Fig. 12. Polyphase structure from Fig. 11 after modifications.

$(W_M^{k(N-1)/2})^2 = W_M^{k(N-1)}$ between IDFT and DFT is equal to one and the output signals of the DFT operation are identical to the input signals of the IDFT scaled by the factor M. The IDFT and DFT can, therefore, be omitted in Fig. 9 and we obtain the structure shown in Fig. 10, where we have already taken into consideration that subband signals delayed by $M/2$ samples with respect to each other can be decimated together.

The MDFT filter bank guarantees PR if the following constraints on the polyphase filters are satisfied:

$$G_k(z) \cdot \overline{G}_k(z) + G_{k+M/2}(z) \cdot \overline{G}_{k+M/2}(z) = \frac{2}{M} z^{-\alpha}, \quad k = 0, \cdots, M/2 - 1. \tag{29}$$

B. Analysis and Synthesis Filters of Length $N = r \cdot M + s$

In the general case, $N = r \cdot M + s$ with $r \in \mathbb{N}$ and $0 \le s < M$, the derivation of the constraints on the polyphase filters for PR is slightly more complicated since the output signal of the DFT differs from the scaled input signal of the IDFT because of the multiplication with $W_M^{k(N-1)} = W_M^{k(s-1)}$ in the kth band. This multiplication can be transferred after the DFT operation by exploiting the effect of a frequency shift on the DFT

$$\text{DFT}\{\tilde{y}(k)\} = \text{DFT}\left\{W_M^{-k(s-1)} y(k)\right\} = x((k-s+1))_M$$

with

$$\text{DFT}\{\tilde{y}(k)\} = \tilde{x}(k)$$

and

$$\text{DFT}\{y(k)\} = x(k). \tag{30}$$

Here, $((k-s+1))_M$ denotes "$(k-s+1)$ modulo M."

In order to apply (30) to the filter bank in Fig. 9, we have to interpret $\tilde{y}(k)$ as the kth output signal of the IDFT, $y(k)$ as the kth input signal of the DFT, and $x(k-s+1)$ as the $(k-s+1)$th output signal of the DFT. This way, we obtain the filter bank depicted in Fig. 11.

The type-3 polyphase filters $\overline{G}_k(z)$ can be expressed by type-1 polyphase filters

$$\begin{aligned} \overline{G}_0(z) &= G_0(z) \\ \overline{G}_k(z) &= z^{-1} G_{M-k}(z), \quad k = 1, \cdots, M-1. \end{aligned} \tag{31}$$

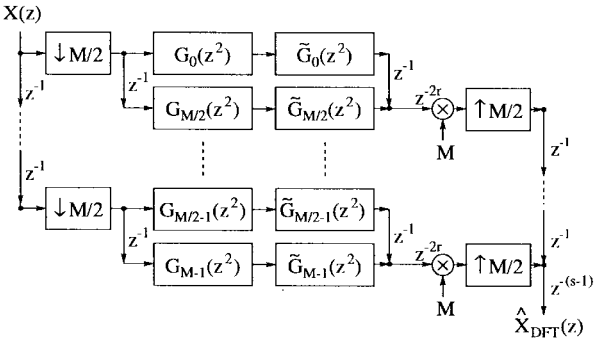

Fig. 13. Polyphase structure with joint subsampling.

As we use a linear-phase low-pass filter $H_0(z)$, exactly two polyphase filters depend on each other [5]

$$g_k(m) = \begin{cases} g_{s-1-k}(r-m), & k < s \\ g_{M+s-1-k}(r-1-m), & k \ge s \end{cases} \tag{32}$$

or in the z domain

$$\tilde{G}_k(z) = G_k^*(z^{-1}) = z^r \begin{cases} G_{s-1-k}(z), & k < s \\ z^{-1} G_{M+s-1-k}(z), & k \ge s. \end{cases} \tag{33}$$

Taking (31) and (33) into account, we can express $\overline{G}_k(z)$ as follows:

$$\begin{aligned} \overline{G}_{M-s+1+k}(z) &= z^{-1} G_{s-1-k}(z) \\ &= z^{-r-1} \tilde{G}_k(z), \quad k \le s-2 \\ \overline{G}_0(z) &= G_0(z) = z^{-r} \tilde{G}_{s-1}(z) \\ \overline{G}_{-s+1+k}(z) &= z^{-1} G_{M-s-1-k}(z) \\ &= z^{-r} \tilde{G}_k(z), \quad s \le k < M. \end{aligned}$$

Inserting these modifications in Fig. 11 and omitting the IDFT and DFT, we attain the structure shown in Fig. 12.

Using the fact that subband signals delayed by $M/2$ samples with respect to each other can be subsampled together, we get the simplified structure in Fig. 13.

Hence, the condition for PR on the polyphase filters is

$$G_k(z)\tilde{G}_k(z) + G_{k+M/2}(z)\tilde{G}_{k+M/2}(z) = \frac{2}{M}. \tag{34}$$

It is equivalent to the condition for PR for cosine-modulated filter banks given in [2], [4], and [5]. Consequently, prototypes

TABLE I
PROTOTYPES OF THE LENGTH $N = 4 \cdot M$ FOR $M = 4, 8, 16, 32$ WITH ABOUT 40-dB STOPBAND ATTENUATION DESIGNED ACCORDING TO [20]; $p(-n) = p(n)$

M	4	8	16	32		32
p(0.5)	-7.9750e-04	2.8579e-04	2.3414e-04	1.7597e-04	p(32.5)	-1.5402e-02
p(1.5)	2.6285e-03	-9.6323e-04	-2.5732e-05	1.4587e-04	p(33.5)	-1.4508e-02
p(2.5)	-1.3793e-02	2.1756e-03	-6.7042e-04	7.7278e-05	p(34.5)	-1.2965e-02
p(3.5)	-4.5462e-02	-2.0473e-03	-1.7186e-03	-4.7434e-05	p(35.5)	-1.0706e-02
p(4.5)	-2.5686e-02	-4.2371e-03	3.2115e-03	-2.3056e-04	p(36.5)	-7.7341e-03
p(5.5)	1.2283e-01	-9.7179e-03	1.8281e-03	-4.7694e-04	p(37.5)	-4.1261e-03
p(6.5)	3.7717e-01	-2.1950e-02	1.1193e-04	-7.7296e-04	p(38.5)	1.1663e-04
p(7.5)	5.8287e-01	-3.0353e-02	-1.6350e-03	-1.1064e-03	p(39.5)	4.8549e-03
p(8.5)		-2.7395e-02	-3.3400e-03	1.8466e-03	p(40.5)	1.1316e-02
p(9.5)		-5.6531e-03	-5.2890e-03	1.5989e-03	p(41.5)	1.9210e-02
p(10.5)		4.3875e-02	-7.4924e-03	1.2171e-03	p(42.5)	2.7653e-02
p(11.5)		1.2112e-01	-9.4247e-03	7.3528e-04	p(43.5)	3.6831e-02
p(12.5)		2.1587e-01	-1.7610e-02	1.8961e-04	p(44.5)	4.6508e-02
p(13.5)		3.1088e-01	-2.0427e-02	-3.9292e-04	p(45.5)	5.6644e-02
p(14.5)		3.8835e-01	-2.2681e-02	-9.4548e-04	p(46.5)	6.7397e-02
p(15.5)		4.3248e-01	-2.3336e-02	-1.4464e-03	p(47.5)	7.8636e-02
p(16.5)			-2.1549e-02	-1.9239e-03	p(48.5)	9.0353e-02
p(17.5)			-1.6793e-02	-2.4456e-03	p(49.5)	1.0236e-01
p(18.5)			-8.2138e-03	-3.0643e-03	p(50.5)	1.1442e-01
p(19.5)			4.7790e-03	-3.7759e-03	p(51.5)	1.2642e-01
p(20.5)			2.3435e-02	-4.4813e-03	p(52.5)	1.3823e-01
p(21.5)			4.6838e-02	-5.1363e-03	p(53.5)	1.4975e-01
p(22.5)			7.4182e-02	-5.6760e-03	p(54.5)	1.6088e-01
p(23.5)			1.0475e-01	-5.9843e-03	p(55.5)	1.7146e-01
p(24.5)			1.3751e-01	-9.9879e-03	p(56.5)	1.8113e-01
p(25.5)			1.7117e-01	-1.1741e-02	p(57.5)	1.8994e-01
p(26.5)			2.0426e-01	-1.3107e-02	p(58.5)	1.9772e-01
p(27.5)			2.3523e-01	-1.4291e-02	p(59.5)	2.0433e-01
p(28.5)			2.6207e-01	-1.5094e-02	p(60.5)	2.0976e-01
p(29.5)			2.8379e-01	-1.5581e-02	p(61.5)	2.1396e-01
p(30.5)			2.9896e-01	-1.5852e-02	p(62.5)	2.1682e-01
p(31.5)			3.0675e-01	-1.5814e-02	p(63.5)	2.1831e-01

designed for an M-channel cosine-modulated filter bank can be applied to a $2M$-channel MDFT filter bank if their impulse responses are scaled by $\sqrt{2}$. Furthermore, the lattice structure for the polyphase filters proposed in [2] can be used, too.

The design of a prototype filter $P(z)$ leading to PR has to be done via nonlinear optimization routines. Design methods can be found in [2], [19], and [20]. Coefficients for prototypes of length $N = 4 \cdot M$ with about 40-dB stopband attenuation resulting from the design method in [20] are given in Table I.

For prototype filters of length $N = 2 \cdot M$, we can use the closed-form expression derived by Malvar as the extended lapped transform (ELT). In our notation the zero-phase prototype filter writes

$$p(n) = -\frac{\sqrt{2}}{16} + \frac{1}{8}\cos\left(\frac{\pi}{2M}\cdot(2n+2M)\right), \quad n = -M+0.5, \cdots, M-0.5. \quad (35)$$

Fig. 14 shows the bifrequency plane of an 8-channel MDFT filter bank using the ELT prototype filter. There are no linear distortions or alias spectra.

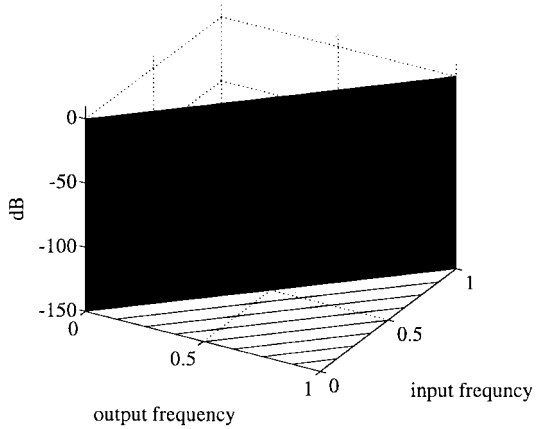

Fig. 14. Bifrequency plane for an 8-channel MDFT filter bank using the prototype from Table I, which guarantees PR.

V. PROCESSING OF REAL-VALUED SIGNALS

Up to now, we have assumed complex valued input sequences and have shown that the MDFT filter bank offers a very efficient realization in this case. However, in practical applications, the input signals are often real valued. In this case we can eliminate M redundant channels in Fig. 4. Because of (13), $y_k^{(R)}(m)$ equals $\pm y_{M-k}^{(R)}(m)$ and $y_k^{(I)}(m)$ equals $\mp y_{M-k}^{(I)}(m)$ for real-valued input signals. The lowpass channel $y_0^{(I)}(m)$ is identical to zero and so is one of

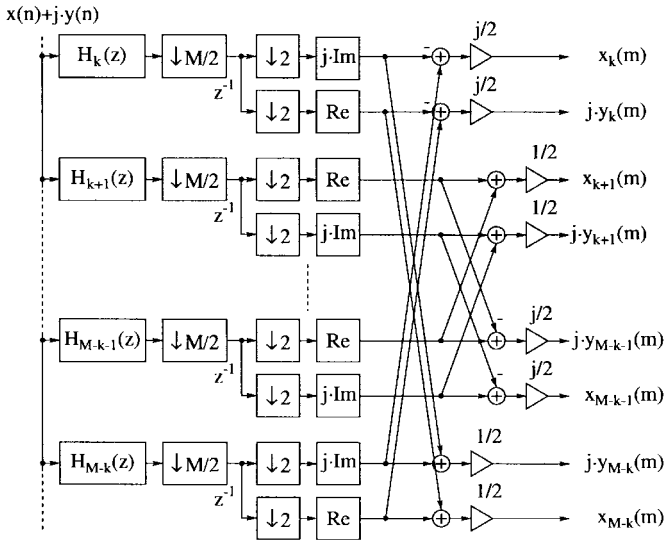

Fig. 15. MDFT filter bank with normal subband signal mapping: the real (imaginary) part of the subband signals is caused by the real (imaginary) part of the input signal.

the subband signals $y^{(R)}_{M/2}(m)$ and $y^{(I)}_{M/2}(m)$ depending of the filter length. All in all, M of the $2M$ subband signals can be omitted as they do not yield further information. For $k = 1, \cdots, M/2-1$, the subband signals $y^{(R)}_k(m)$ and $y^{(I)}_k(m)$ occupy the same frequency range.

If there is more than one signal to be processed, we can build a complex input signal from two independent real signals by mapping them into the real and imaginary parts, respectively. In order to encode the signals separately, we wish to have a mapping of the input signal into the subbands in such a way that the real (imaginary) part of the subband signals is caused by the real (imaginary) part of the input signal. However, the subband signals of the MDFT filter bank contain information of both the real and the imaginary part of the input signal [see (17)–(20)]. The mapping of the real and imaginary part of the input signal into the subbands does not depend on the sampling-rate decimation. We therefore start from (11) and (12), and show for odd-length prototype filters [upper sign in (11) and (12)] that the desired mapping can be obtained by adding or substracting the kth and $(M-k)$th subband signal and multiplying by $1/2$ or $\pm j/2$

$$\tfrac{1}{2}(\mathrm{Re}\{h_k(n)*x(n)\}+\mathrm{Re}\{h_{M-k}(n)*x(n)\}) = \tfrac{1}{2}[h_k(n)+h_{M-k}(n)]*x_R(n) \quad (36)$$

$$-\frac{j}{2}(\mathrm{Re}\{h_k(n)*x(n)\}-\mathrm{Re}\{h_{M-k}(n)*x(n)\}) = \tfrac{1}{2}[h_k(n)-h_{M-k}(n)]*j\cdot x_I(n) \quad (37)$$

$$\tfrac{1}{2}(j\mathrm{Im}\{h_k(n)*x(n)\}+j\mathrm{Im}\{h_{M-k}(n)*x(n)\}) = \tfrac{1}{2}[h_k(n)+h_{M-k}(n)]*j\cdot x_I(n) \quad (38)$$

$$\frac{j}{2}(j\mathrm{Im}\{h_k(n)*x(n)\}-j\mathrm{Im}\{h_{M-k}(n)*x(n)\}) = \tfrac{1}{2}[h_k(n)-h_{M-k}(n)]*x_R(n). \quad (39)$$

These operations are included in the analysis filter bank in Fig. 15. The complex input signal is a combination of two real input signals $x(n)$ and $y(n)$ [note that $x(n)$ and $y(n)$ correspond to $x_R(n)$ and $x_I(n)$, respectively, in the above equations]. Due to the butterflies which carry out the above equations, we obtain M real (imaginary) subband signals caused by the real (imaginary) part of the input sequence. For even-length prototypes additions and subtractions have to be swapped.

VI. Comparison of MDFT Filter Banks and Cosine-Modulated Filter Banks

Cosine-modulated filter banks with PR are extensively discussed in literature, e.g., [2], [5], [16]. The M analysis and synthesis filters are derived from a linear-phase low-pass prototype $h(n)$ of the bandwidth π/M (including positive and negative frequencies) in the following way:

$$h_k(n)=2h(n)\cos\left((2k+1)\frac{\pi}{2M}\left(n-\frac{N-1}{2}\right)+(-1)^k\frac{\pi}{4}\right),$$

$$f_k(n)=2h(n)\cos\left((2k+1)\frac{\pi}{2M}\left(n-\frac{N-1}{2}\right)-(-1)^k\frac{\pi}{4}\right),$$

$$n=0,\cdots,N-1, \quad k=0,\cdots,M-1.$$

When comparing MDFT filter banks with cosine-modulated filter bank, we can state the following differences.

1) Taking an M-channel filter bank in both cases and assuming a complex-valued input signal, the prototype filter for the cosine-modulated filter bank has half the bandwidth of that for the MDFT filter bank. In order to obtain the same stopband attenuation, the prototype filter for the cosine-modulated filter bank must have approximately twice the length of that for the MDFT filter bank. Therefore, an M-channel MDFT filter bank has half of the propagation delay time of an M-channel cosine-modulated filter bank which is important for real-time applications. Prototypes for a $2M$-channel MDFT filter bank and for an M-channel cosine modulated filter bank are the same.
2) For real-valued input signals, the MDFT filter bank has a similar structure as the filter bank derived by Lin and Vaidianathan [4], consisting of an alternate sine and cosine modulation (in case of a real-valued input signal, taking the real and imaginary part of the subband signals is equivalent to taking the real and imaginary part of the analysis filters' impulse responses). When comparing their filter bank to a cosine-modulated filter bank as described above in terms of the attainable coding gain, they found out that similar results were obtained with their $2M$-channel filter bank as with an M-channel cosine-modulated filter bank. Thus, in order to obtain a coding gain comparable with that of an M-channel cosine-modulated filter banks when processing real valued input signals, we also need a $2M$-channel MDFT filter bank. Both filter banks are then of the same complexity and provide similar propagation delays.
3) In the perfect-reconstruction case, the cosine-modulated filter bank has a linear-phase prototype but nonlinear-phase analysis and synthesis filters. When treating finite-length signals as, e.g., images, this is unfavorable since we cannot use symmetric extension methods to obtain a

support preservative analysis/synthesis system. Instead, we either have to use cyclic convolution, which is sensitive to quantization errors due to the discontinuity of the input signal across the boundaries [22], [23], or we have to optimize the analysis/synthesis filters for the boundaries [24], [25]. The last method has the disadvantage that the boundary filters are no longer cosine-modulated versions of a low-pass prototype.

The MDFT filter bank has linear-phase analysis and synthesis filters but it also contains delay elements within the analysis and synthesis filter bank. Due to the last fact, symmetric extension methods as discussed in [26]–[28] cannot be directly applied to MDFT filter banks but have to be adapted (see [29] and [30]).

4) We have pointed out in Section V that the MDFT filter bank has a different mapping of the subband signals than the cosine-modulated filter bank. With the structure from Fig. 15, we can also obtain a normal mapping, where the real (imaginary) part of the subband signals is caused by the real (imaginary) part of the input signal. This can be used when treating audio stereo signals which can be transformed jointly with the MDFT filter bank [31].

   The MPEG-1 audio standard [32] uses a 32-channel cosine-modulated filter bank to split an audio signal into subbands. A psychoacoustic model takes masking effects of the human ear [33] into account. Both parts are performed separately for the left and right channel of a stereo signal. It has turned out that similar results can be obtained for layer 1 when substituting the cosine-modulated filter bank by a 32-channel MDFT filter bank according to Fig. 15 [31]. The left and right channel can then be transformed into the subbands jointly but both channels are coded separately. The coding algorithm has to be adapted to the frequency bands of the MDFT filter bank. Fig. 16 shows the signal-to-noise-ratio (SNR) of the reconstructed signal for different bitrates using the original MPEG-1 layer-1 algorithm and the one adapted to the 32-channel MDFT filter bank. The SNR does not take any masking effects into account. Hearing tests have turned out that there is hardly any difference between both filter banks. However, the MDFT filter bank only leads to half the propagation delay due to Point 1 and is preferable for real-time applications.

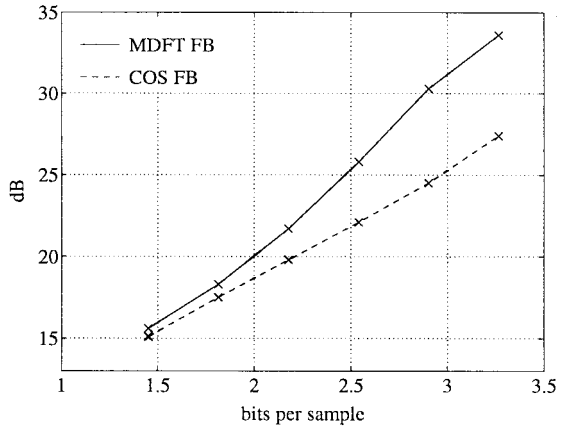

Fig. 16. SNR of a reconstructed music example for an audio coder according to MPEG-1 layer 1 using a 32-channel cosine-modulated filter bank and MDFT filter bank.

VII. Conclusion

In this paper, we have shown that the recently introduced MDFT filter bank consists of linear-phase analysis and synthesis filters which are derived from an appropriate zero-phase prototype filter. The linear phase of all filters is one of the key features of the filter bank. Another important property is the structure inherent alias cancellation: all odd alias spectra disappear automatically during the synthesis. This feature directly leads to the design of a filter bank with almost PR.

Furthermore, as another main result of this paper, we have derived the conditions on the prototype filter for PR of the MDFT filter bank. They are identical to those for cosine-modulated filter banks. Thus, the same design methods can be used for the prototype filter.

Compared to cosine-modulated filter banks, the MDFT filter bank shows some similarities and some differences: the MDFT filter bank has a different mapping of the input signal into the subbands and is particularly suitable for complex signal processing. Assuming the same number of channels, i.e., the same decimation factor, the MDFT filter bank needs half of the propagation delay time of the cosine modulated filter bank. In [7] and [11], it has been shown that the computational complexities of both kinds of filter banks are comparable. Altogether, the MDFT filter bank is an alternate solution which may have certain advantages in some applications.

References

[1] T. A. Ramstad, "Cosine-modulated analysis-synthesis filterbank with critical sampling and perfect reconstruction," in *Proc. Int. Conf. Acoustics, Speech and Signal Processing*, Toronto, Canada, May 1991, pp. 1789–1792.

[2] R. D. Koilpillai and P. P. Vaidyanathan, "Cosine-modulated FIR filter banks satisfying perfect reconstruction," *IEEE Trans. Signal Processing*, vol. 40, pp. 770–783, Apr. 1992.

[3] R. Gopinath and C. Burrus, "Theory of modulated filter banks and modulated wavelet tight frames," in *Proc. IEEE Int. Conf. Acoustics, Speech, and Signal Processing*, Minneapolis, MN, Apr. 1993, pp. 169–172.

[4] Y. Lin and P. P. Vaidyanathan, "Linear phase cosine modulated maximally decimated filter banks with perfect reconstruction," *IEEE Trans. Signal Processing*, vol. 43, pp. 2525–2539, Nov. 1995.

[5] T. Q. Nguyen and R. D. Koilpillai, "The theory and design of arbitrary-length cosine-modulated filter banks and wavelets, satisfying perfect reconstruction," *IEEE Trans. Signal Processing*, vol. 44, pp. 473–483, Mar. 1996.

[6] M. G. Bellanger and J. L. Daguet, "TDM-FDM transmultiplexer: Digital polyphase and FFT," *IEEE Trans. Commun.*, vol. COM-22, pp. 1199–1204, Sept. 1974.

[7] N. J. Fliege, "Computational efficiency of modified DFT-polyphase filter banks," in *Proc. 27th Asilomar Conf. Signals, Systems and Computers*, Asilomar, Nov. 1993, pp. 1296–1300.

[8] ——, "Modified DFT polyphase SBC filter banks with almost perfect reconstruction," in *Proc. IEEE Int. Conf. Acoustics, Speech and Signal Processing*, Adelaide, Australia, Apr. 1994, vol. 2, pp. 149–152.

[9] T. Karp and N. J. Fliege, "MDFT filter banks with perfect reconstruction," in *Proc. IEEE Int. Symp. Circuits and Systems*, Seattle, WA, May 1995, pp. 744–747.

[10] N. J. Fliege, *Multirate Digital Signal Processing.* Chichester, U.K.: Wiley, 1994.

[11] T. Karp and N. J. Fliege, "Computational efficient realization of MDFT filter banks," in *Proc. EURASIP European Signal Processing Conf.*, Trieste, Italy, Sept. 1996, pp. M83–1186.

[12] J. H. Rothweiler, "Polyphase quadrature filters—A new subband coding technique," in *Proc. IEEE Int. Conf. Acoustics, Speech, and Signal Processing*, 1983, pp. 1280–1283.
[13] J. H. Nussbaumer and M. Vetterli, "Computationally efficient QMF filter banks," in *Proc. IEEE Int. Conf. Acoustics, Speech, and Signal Processing*, San Diego, CA, Mar. 1984.
[14] J. Masson and Z. Picel, "Flexible design of computationally efficient nearly perfect QMF filter banks," in *Proc. IEEE Int. Conf. Acoustics, Speech, and Signal Processing*, Tampa, FL, 1985, pp. 541–544.
[15] T. Nguyen, "Near-perfect-reconstruction pseudo-QMF banks," *IEEE Trans. Signal Processing*, vol. 42, pp. 64–75, Jan. 1994.
[16] P. P. Vaidyanathan, *Mulitrate Systems and Filter Banks.* Englewood Cliffs, NJ: Prentice-Hall, 1993.
[17] N. J. Fliege and G. Rösel, "Optimized design of MDFT filter banks," in *Proc. Int. Conf. Digital Signal Processing*, Limassol, Cyprus, June 1995, pp. 171–176.
[18] R. E. Crochiere and L. R. Rabiner, *Multirate Digital Signal Processing.* Englewood Cliffs, NJ: Prentice-Hall, 1983.
[19] T. Nguyen, "A quadratic-constrained least-squares approach to the design of digital filter banks," in *Proc. IEEE Int. Symp. Circuits and Systems*, San Diego, CA, May 1992, pp. 1344–1347.
[20] ———, "Digital filter banks design—Quadratic-constrained formulation," *IEEE Trans. Signal Processing*, vol.43, pp. 2103–2108, Sept. 1995.
[21] H. S. Malvar, *Signal Processing with Lapped Transforms.* Norwood, MA: Artech House, 1992.
[22] J. Woods and S. O'Neil, "Subband coding of images," *IEEE Trans. Acoust., Speech, Signal Processing*, vol. ASSP-34, pp. 1278–1288, Oct. 1986.
[23] M. J. T. Smith and S. L. Eddins, "Analysis/sythesis techniques for subband image coding," *IEEE Trans. Acoust., Speech, Signal Processing*, vol. 38, pp. 1446–1456, Aug. 1990.
[24] C. Herley and M. Vetterli, "Orthogonal time-varying filter banks and wavelet packages," *IEEE Trans. Signal Processing*, vol. 42, pp. 2650–2663, Oct. 1994.
[25] A. Mertins, "Time-varying and support preservative filter banks: Design of optimal transition and boundary filters via SVD," in *Proc. IEEE Int, Conf, Acoust., Speech, Signal Processing*, Detroit, MI, May 1995, pp. 1316–1319.
[26] C. M. Brislawn, J. N. Bradley, and V. Faber, "Reflected boundary conditions for multirate filter banks," in *Proc. IEEE Int. Symp. Time-Frequency and Time-Scale Analysis*, 1992, pp. 307–310.
[27] S. A. Martucci and R. M. Mersereau, "The symmetric convolution approach to the nonexpansive implementation of filter banks for images," in *Proc. IEEE Int. Conf. Acoustics, Speech and Signal Processing*, 1993, pp. 65–68.
[28] L. Chen, T. Q. Nguyen, and K. P. Chan, "Symmetric extension methods for *M*-channel linear-phase perfect reconstruction filter banks," *IEEE Trans. Signal Processing*, vol. 43, pp. 2505–2511, Nov. 1995.
[29] T. Karp, A. Mertins, and N. J. Fliege, "Processing finite-length signals with MDFT filter banks," in *Proc. 15th GRETSI Symp. Signal and Image Processing*, Jes les Pins, France, Sept. 1995, pp. 749–752.
[30] T. Karp, J. Kliewer, A. Mertins, and N. J. Fliege, "Processing arbitrary-length signals with MDFT filter banks," in *Proc. IEEE Int. Conf. Acoustics, Speech, and Signal Processing*, Atlanta, GA, May 1996, pp. 1479–1482.
[31] T. Karp, R. Adloff, and N. J. Fliege, "Application of MDFT filter banks to audio coding," in *Proc. European Workshop on Digital Multirate Signal Processing and Applications*, Hamburg, Germany, Mar. 1996.
[32] *Coding of Moving Pictures and Associated Audio for Digital Storage Media up to about 1.5 Mbits/s, Part 3, Audio*, ISO/IEC International Standard ISO 11172-3, 1992.
[33] E. Zwickel and H. Fastl, *Psychoacoustics.* New York: Springer-Verlag, 1990.

Tanja Karp (M'98) was born in Germany in 1969. She received the Dipl.-Ing. degree in electrical engineering and the Dr.-Ing. degree from Hamburg University of Technology, Germany, in 1993 and 1997, respectively.

In 1995 and 1996, she spent two months as a Visiting Researcher at the Signal Processing Department, ENST Paris, France, and also at the Multirate Signal Processing Group, University of Wisconsin at Madison, working on modulated filter banks. Since 1997, she has been with Mannheim University, Mannheim, Germany, as a Research and Teaching Assistant. Since 1998, she has been a Guest Lecturer at Freiburg University. Her research interests include multirate signal processing, filter banks, audio coding, images coding, multicarrier modulation, and signal processing for communications.

N. J. Fliege (M'89–SM'90) recieved the Dipl.-Ing. and Dr.-Ing. degrees in 1971, both from the University of Karlsruhe, Germany.

He was an Associate Professor at the University of Karlsruhe since 1978. In 1980, he joined ESIEE, Paris, France, as an Associate Professor. From 1982 to 1996, he was a Full Professor and Head of the Telecommunication Institute, Hamburg University of Technology, Hamburg, Germany. Since 1996, he has been a Full Professor of Electrical Engineering and Computer Technology at the University of Mannheim, Germany. Since 1968, Dr. Fliege has been engaged in research work in fields like active filters, digital filters, communication circuits and software, digital audio, and multirate digital signal processing. In addition, he served as a Department Chairman and as Head of a research center. He also founded a company which produces electronic equipment. He has published about 100 papers, most of them in international magazines and conference proceedings, and four books, one being *Multirate Digital Signal Processing* (New York: Wiley, 1994).

Dr. Fliege has received several national and international awards. In 1997, he received the honorary doctorate from the University of Rostock, Germany. He is a member of EURASIP and VDE (Germany).